Combustion and Flame 188 (2018) 90–93

Contents lists available at ScienceDirect

Combustion and Flame

journal homepage: www.elsevier.com/locate/combustflame

Brief Communications

Transition condition and control mechanism of subatmospheric flame spread rate over horizontal thin paper sample

Jun Fang[a], Xuan-ze He[a], Kai-yuan Li[b,c,*], Jing-wu Wang[a], Yong-ming Zhang[a]

[a] State Key Laboratory of Fire Science, University of Science and Technology of China, Hefei, Anhui 230026, PR China
[b] Univ. Lille, UMR 8207, UMET, Unité Matériaux et Transformations, F 59 000 Lille, France
[c] Department of Civil Engineering, School of Engineering, Aalto University, 02150 Espoo, Finland

ARTICLE INFO

Article history:
Received 7 April 2017
Revised 18 June 2017
Accepted 8 September 2017

ABSTRACT

The horizontal flame spread over paper samples was investigated using a subatmospheric cabin with varied O_2 concentration. The 25 kPa is found to be a clear turning point for the flame illumination and structure, radiative heat flux and flame spread rate (FSR), which leads to the transition boundary between the extinction limits and power law regions. In the extinction limits (non-linear) region below 25 kPa, the oxygen partial pressure is low with a small *Da* number. Consequently, the flame spread is gas phase kinetics controlled, resulting in low burning rate, low radiative heat loss and weak buoyancy, and thus the FSR is more sensitive to the oxygen concentration while less sensitive to the ambient pressure. In the power law (linear) region above 25 kPa, in contrast, the oxygen partial pressure is high and the *Da* number is large, and the flame spread is heat transfer controlled, which weakens the dependence of FSR on oxygen concentration and enhances the dependence on air pressure.

1. Introduction

Subatmospheric flame spread is crucial for understanding of the fire behaviors with low buoyancy in microgravity. Olson et al. [1] studied the opposed flow flame spread over thin cellulose material near the extinction limits in microgravity and obtained the flammability map for near extinction limits in flame spread. Jie et al. [2] investigated the effects of subatmospheric pressure and sample width on the characteristics of horizontal flame spread over wood sheets. Frey and T'ien [3] studied the horizontal flame spread in various conditions (oxygen concentration and pressure) in a quiescent subatmospheric environment. They claimed that the power law relation could only correlate the data away the extinction limits. The correlation employing the infinite reaction rate is expressed as [4]:

$$V_f \propto (pY_{O_2}^m)^{\phi} \tag{1}$$

where V_f is the FSR, p the ambient pressure, Y_{O_2} the O_2 concentration. The exponent index, m, is found as respective 3.1 and 1 for PMMA and paper while ϕ approaches unity for both materials [3,4]. Nevertheless, Eq. (1) ignored the near extinction limits condition in the previous research [3], therefore, a global model is demanded for the subatmospheric FSR.

To come up with a global model, the transition boundary of near extinction limits and power law regions should first be identified. However, no available work focused on this boundary by far as well as the control mechanism of flame spread in different regions.

In this paper, the horizontal flame spread over a paper sample was investigated experimentally using a subatmospheric cabin with an adjustable O_2 concentration. The transition boundary, flame behaviors, flame temperature and radiative heat flux under varied O_2 concentration and pressure were obtained. The literature data are also compared and involved in the analysis. The effects of pressure and O_2 concentration on FSR were analyzed in depth with a global correlation developed.

2. Experimental setup

A cylindrical subatmospheric cabin with a diameter of 50 cm and a length of 40 cm was used, in which the inner pressure can be varied from 0.3 to 100 kPa (±0.01 kPa). Pure O_2 is mixed with air to adjust the O_2 concentration from 21% to 80% in mole fraction.

The experimental setup is shown in Fig. 1. The paper samples were 12 cm long, 2 cm wide and 0.012 cm thick and fixed using two parallel stainless steel plates. A coil heater was used to provide a

* Corresponding author: Department of Civil Engineering, School of Engineering, Aalto University, 02150 Espoo, Finland.
E-mail addresses: kaiyuan.li@aalto.fi, stevelikai@126.com (K.-y. Li).

https://doi.org/10.1016/j.combustflame.2017.09.010
0010-2180/

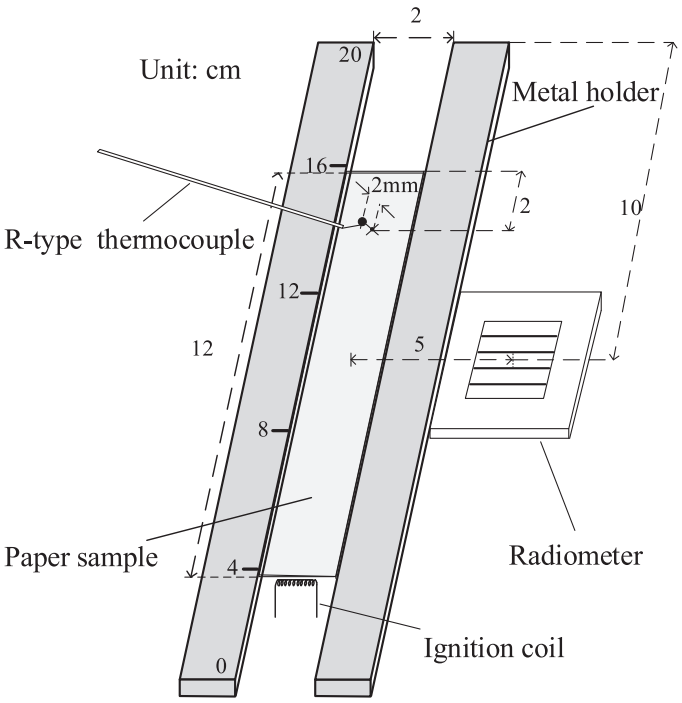

Fig. 1. Top view of the experimental setup.

Table 1
Varied pressures at 43% O_2. (LOC: Limiting oxygen concentration).

No.	Pressure (kPa)	O_2 (%)
1	10	43 (LOC)
2	15	43
3	20	43
4	25	43
5	30	43
6	35	43
7	40	43
8	45	43

6 A current to ignite the paper sample, which would be stopped immediately once the flame spread began.

To avoid the heat loss caused by intrusive measurements for flame spread near the extinction limits, only one R-type thermocouple with a diameter of 0.1 mm (±0.1 K) was installed to obtain the local flame temperature. The thermocouple was positioned 2 cm to the paper rear side and 2 mm above the paper sample. The thermocouple can quench the flames with low heat release rates, hence, the temperature data were very treasurable. Moreover, a radiometer parallel to the paper sample at the same horizontal level was placed 5 cm away the sample center-point, which was used as a reference to reflect the local flame incident radiative heat flux. The flame spread process was recorded using two Canon cameras (ISO 2500, shutter speed 1/30, F5.6, 1920 × 1080@30 fps) from the top and side views. The experimental conditions are listed in Tables 1 and 2.

3. Experimental results and discussion

Figure 2 shows the flame spread images against oxygen concentration and ambient pressure above the flammability limits. It is noted that below 25 kPa the flame is lightless blue and elliptical with a longitudinal symmetry structure. Specially, only when pressure above 25 kPa, the yellow flame will be shown. As the pressure increases, below 25 kPa, the flame size increases significantly, whereas above 25 kPa, owing to the increasing buoyancy, the flame height increases noticeably and establishes a longitudinal asymmetry structure. Moreover, when the ambient pressure exceeds 25 kPa, with increasing pressure and oxygen concentration, the flame turns more yellow and luminous.

Table 2
Varied pressures via increasing oxygen concentration.

No.	Pressure (kPa)	O_2 (%)
1	10	43 (LOC), 45, 47, 49, 51
2	20	29 (LOC), 31, 33, 35, 37
3	25	27 (LOC), 29, 31, 33, 35
4	30	25 (LOC), 27, 29, 31, 33
5	50	21, 23, 25, 27, 29
6	70	21, 23, 25, 27, 29
7	90	21, 23, 25, 27, 29

Figure 3(a) shows the radiative heat flux 5 cm away from the sample against oxygen concentration and pressure while Fig. 3(b) shows the radiative heat flux and flame temperature at 43% O_2 against pressure. It can be seen that 25 kPa is clearly a transition point for the increase rate of radiative heat flux. Furthermore, both the oxygen concentration and pressure have positive effects upon the increase of radiative heat flux, while at the same oxygen concentration the flame temperature has a significant decrease with increasing pressure. It is because that with increasing oxygen concentration and pressure the oxygen partial pressure increases, the combustion becomes stronger with a higher heat release rate, so the radiative heat feedback significantly increases. Moreover, at the same oxygen concentration, with the increasing pressure, the production of soot particles increases, as the soot yield Y_s is inversely proportional to the soot formation time and hence in diffusion flames it follows the second order of ambient pressure [5]. Meanwhile, the gaseous combustion products of H_2O and CO_2 increase linearly with pressure. Thus the radiation heat loss increases and the flame temperature decreases.

Figure 4(a) shows $V_f d/W$ against oxygen concentration and ambient pressure using the experimental data in this work and the work of Frey and T'ien [3], where the extinction, upper and lower limits are given. It is seen that in the extinction limit regions below 25 kPa, the FSR increases non-linearly with the pressure, while in the classical power law region above 25 kPa the FSR increases linearly with the pressure. Figure 4(b) presents the fitting of $(V_f d/W)/Y_{O_2}^{1.4}$ and $(V_f d/W)/Y_{O_2}$ against ambient pressure.

Therefore, the global correlation of FSR involving the two regions is expressed as Eq. (2):

$$\begin{cases} V_f \propto Y_{O_2}^{1.4} p^{0.66} & (p < 25\,\text{kPa}) \\ V_f \propto Y_{O_2} p & (p > 25\,\text{kPa}) \end{cases} \tag{2}$$

In the literature, the FSR has been justified to linearly correlate to the flame heat feedback, which can be calculated using Eq. (3) [6]:

$$V_f = \frac{\dot{q}''_{fb}\delta_f}{\rho c_p d(T_{ig} - T_s)} \tag{3}$$

Here, $\dot{q}''_{fb}$ is the net heat flux to the sample surface, $\dot{q}''_{fb} = \dot{q}''_f - \dot{q}''_{loss}$, where $\dot{q}''_f$ is the flame incident heat flux, which is proportional to the overall reaction rate $\dot{m}'''_F = \rho_g A_0 Y_F^n Y_{O_2}^m \exp(-E/RT)$ where the exponent m is approximately 1.5 [7]. The heat loss $\dot{q}''_{loss}$ mainly includes the radiation losses from the flame and the sample surface. δ_f is the distance between flame front and ignition point (preheating length), d the sample thickness, ρ the sample density, c_p the sample specific heat, T_{ig} the ignition temperature, T_s the surface temperature.